Agricultural Water Management 102 (2011) 8–12

Contents lists available at SciVerse ScienceDirect

Agricultural Water Management

journal homepage: www.elsevier.com/locate/agwat

Delineating water management zones in a paddy rice field using a Floating Soil Sensing System

Mohammad Monirul Islam*, Timothy Saey, Eef Meerschman, Philippe De Smedt, Fun Meeuws, Ellen Van De Vijver, Marc Van Meirvenne

Research Group Soil Spatial Inventory Techniques, Department of Soil Management, Faculty of Bioscience Engineering, Ghent University, Coupure 653, 9000 Gent, Belgium

ARTICLE INFO

Article history:
Received 15 July 2011
Accepted 5 October 2011
Available online 29 October 2011

Keywords:
Water infiltration
Apparent electrical conductivity
EM38
Inundated soil
Paddy rice fields

ABSTRACT

Paddy rice fields are kept inundated during most of the growing period. This requirement is challenging to achieve because of the lack of suitable technologies to detect rapidly percolation prone zones within these fields. The objective of this study was to evaluate a methodology to identify water leakage areas to support precision soil–water management at a within-field level. Therefore, a Floating Sensing System (FloSSy) was designed to record the soil apparent electrical conductivity (EC_a) of a paddy field both under dry and inundated conditions using the electromagnetic induction sensor EM38. Comparison of EC_a data sets obtained under inundated and dry conditions showed that the EC_a measurements under inundated condition (EC_a-i) were more strongly related to soil properties due to the absence of variability in soil moisture and the increased stability of the floating sensing platform. Therefore, we proceeded with the EC_a-i measurements and grouped them into two classes using a fuzzy *k*-means classification method. These classes showed significant differences in water infiltration: lower EC_a values represented a higher infiltration rate and vice versa. This effect was attributed to differences in soil texture, more specifically the sand content, and its effect on water retention. It was concluded that an EC_a-i survey with FloSSy allowed the detection of soil heterogeneity linked to downward water fluxes which has a potential to support precision soil–water management in inundated fields.

1. Introduction

The most frequent cultivation system of rice is paddy rice where the fields remain inundated for most of the cropping season. Maintenance of standing water at a recommended depth is crucial to ensure sufficient water availability to the crop. Water losses from an inundated paddy field on a plain landscape like in Bangladesh occur either by evapotranspiration (ET) or by percolation below the rooting zone. Since ET is directly linked to crop production, the most efficient reduction of water loss and dissolved nutrients in paddy fields is to reduce the downward flux (Bouman and Tuong, 2001). Therefore, these fields are typically puddled during land preparation. While the soil is kept saturated, it is ploughed repeatedly to reduce porosity. An extra advantage of puddling is the effective control of weed growth as standing water in the inundated rice fields strongly reduces weed emergence (Yoshida, 1983). However, preventing water losses by drainage from paddy fields remains a challenge for the rice growers. The problem persists as the formation of a homogenously puddled and relatively impermeable layer with an underlying continuous plough pan is complicated by the spatial variability of soil properties, in particular soil texture. A sandy zone within a generally clayey field might create locally less impermeable conditions resulting in unexpectedly large water losses affecting the entire field. If lost water is not refilled, dry zones form inside the field where weeds start to flourish immediately, competing for nutrients. These surface expressions become evident only after the land preparation when paddy rice has already been planted. As a consequence, direct methods for the acquisition of detailed information on soil–water properties before land preparation would be welcome. Therefore, precision agriculture (PA), which aims at adjusting soil management according to the within field soil variability, needs to be considered. Recent technological advances in proximal soil sensing allow the acquisition of high resolution soil information under flooded conditions that can be interpreted to detect the within field variability and serve as a basis for precision soil–water management.

Soil apparent electrical conductivity (EC_a) measured with an electromagnetic induction (EMI) based proximal soil sensor can be interpreted to explain variation in soil properties (Sudduth et al., 1997), like texture (Saey et al., 2009), salinity, bulk density or pore volume (Rhoades et al., 1999) and depth to a clay layer (Saey et al., 2008). However, often the influence of dynamic moisture variation on the measured EC_a (Brevik et al., 2006) obscures the actual source of variation and complicates the detection of soil variation. This

* Corresponding author.
E-mail address: mohammadmonirul.islam@ugent.be (M.M. Islam).

0378-3774/$ – see front matter © 2011 Elsevier B.V. All rights reserved.
doi:10.1016/j.agwat.2011.10.001

masking effect of moisture is eliminated in a flooded environment where variations in EC_a directly reflect changes in soil properties other than soil moisture (Islam et al., 2011a). For inundated paddy fields, the traditionally used dry EC_a survey is also not practical because the surveyor has to wait until the fields are drained. To overcome these limitations, a proximal soil sensing system suited to operate on inundated fields was designed.

The main objective was to assess the applicability of the sensing system to delineate zones related to water percolation losses at a within field scale. Hence, the characterization of a paddy field under inundated and drained conditions and the comparison of both surveys were followed by interpretation of the differences in terms of soil texture and water infiltration.

2. Materials and methods

2.1. Study site

A 1.4 ha paddy field of the Bangladesh Agricultural University in Mymensingh was selected to conduct the study. The field has central co-ordinates 24.7187°N and 90.4293°E and is located in the old floodplain of the river Brahmaputra. The soil was developed on the alluvial deposits of the river and mainly consists of fine sand to silt (Brammer, 1996). Soil survey reported that these floodplain soils of the river Brahmaputra are non-saline (Brammer, 1981). Hence, only rice varieties suitable for non-saline soil conditions are used on these floodplain soils. The field has a wet paddy cultivation history of more than three decades. Puddling of wet soil is the usual practice of land preparation before crop planting.

2.2. The Floating Sensing System

To acquire high resolution soil data on both dry (drained) and inundated field conditions, we developed a mobile soil sensing system called the Floating Sensing System, or FloSSy (Islam et al., 2011b). For this, only non-invasive and non-contact EMI proximal sensors were considered as invasive sensors would fail to obtain acceptable results under inundated conditions and remote sensors would be incapable of acquiring soil information beneath the standing water. Therefore the EM38 (Geonics Limited, Canada) was selected as proximal soil sensor. Moreover, it is a light-weight instrument (about 3.5 kg) and has a small physical dimension (1.05 m × 0.16 m × 0.05 m). The intercoil distance of the EM38 sensor is 1 m. During measurements, an alternating current is passed through a transmitter coil of the sensor, which produces a primary magnetic field. This primary magnetic field induces eddy currents in the soil which create a secondary magnetic field proportional to the strength of the currents. The secondary magnetic field induces again alternating currents in the receiver coil, which is directly related to a depth-weighted average soil EC_a. More technical details and operating principles of the EMI technique can be found in McNeill (1980). Operating the sensor in the vertical orientation, as in this study, results in a depth of influence of about 1.5 m, representing 70% of its accumulated depth response under homogeneous soil conditions. Hence, with a standing water depth of 0.10–0.25 m, influence of the shallow soil material beneath the water layer could be measured.

FloSSy consists of an EM38 kept inside a waterproof housing and placed on a wooden raft (Fig. 1). The waterproof housing was equipped with a GPS receiver on top so that its position indicated the centre of the sensor. A 12 HP vehicle (a paddy field 'power tiller') was used to trail the wooden raft. The georeferenced sensor data were logged and processed *in situ* using a field laptop. More details on FloSSy can be found in Islam and Van Meirvenne (2011).

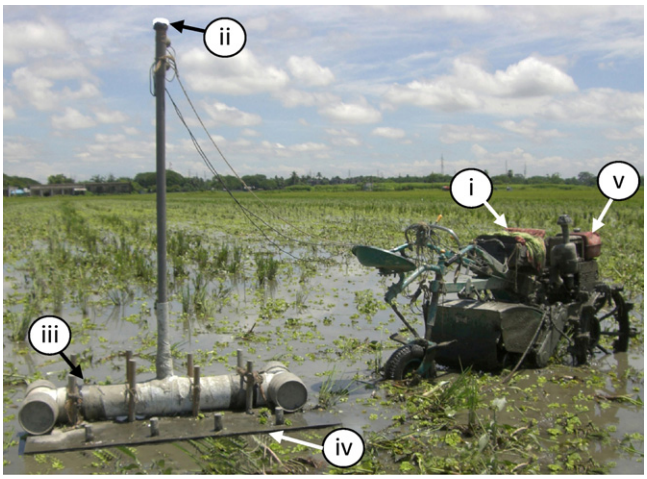

Fig. 1. The Floating Soil Sensing System (FloSSy) during field measurement of EC_a. The different components are indicated as follows: (i) laptop, (ii) GPS, (iii) water proof sensor housing, (iv) floating platform, and (v) the power tiller.

2.3. EC_a survey and data processing

The EC_a survey under dry conditions (EC_a-d) was conducted in July 2009 immediately after the rice harvest. The sensing platform was at 0.12 m above the soil surface to ensure minimal damage to the rice stubbles (commonly used for soil organic matter during land preparation for the next crop). One and a half month later, just before the seasonal planting of rice seedlings, EC_a was measured again under inundated conditions (EC_a-i) with 0.10–0.12 m water standing on the soil surface. Thus the distance above the soil surface was similar in both surveys. Measurements were taken along parallel lines 1 m apart. With a ground speed of approx. 3.6 km h^{-1}, the logging frequency of the system was 4 Hz. Soil temperature was recorded every hour using a bimetal soil temperature sensor pushed into the ground at a depth of 0.25 m below the surface. During both surveys, the soil temperature remained stable at 30 °C. The obtained EC_a measurements were averaged to one value per m^2 and post-corrected for instrumental drift according to the deviation from an initial diagonal measurement across the field. Resulting data were standardized to a reference temperature of 25 °C by (Sheets and Hendrickx, 1995):

$$EC_{a_{25}} = EC_{a_{obs}}(0.4470 + 1.4034 \cdot e^{-T/26.815}) \quad (1)$$

where $EC_{a_{25}}$ is the standardized EC_a values at 25 °C and $EC_{a_{obs}}$ is the observed EC_a values at soil temperature T (°C). In the following part of this paper, all EC_a measurement values refer to the EC_a at 25 °C.

2.4. Variogram analysis and kriging

The structure of the spatial variance of the EC_a measurements was examined through variogram analysis. Omni-directional standardized variograms were computed for EC_a-d and EC_a-i. Both experimental variograms $\gamma(\mathbf{h})$ were best fit with a spherical model ($\gamma(\mathbf{h}) = 0$ if $\mathbf{h} = 0$):

$$\gamma(\mathbf{h}) = \begin{cases} C_0 + C_1 \cdot [1.5(\mathbf{h}/a) - 0.5(\mathbf{h}/a)^3] & \text{if } 0 < \mathbf{h} \le a \\ C_0 + C_1 & \text{if } \mathbf{h} > a \end{cases} \quad (2)$$

where $\mathbf{h}$ is the spatial lag vector, C_0 is the nugget variance, C_1 is the structured variance and a is the range. Afterwards the EC_a data were interpolated to a regular grid with 1 m × 1 m resolution using ordinary point kriging (OK) (Goovaerts, 1997). The mapping software Surfer was used for both variogram analysis and kriging (Golden Software Inc., U.S.A.). The interpolated EC_a-i values were

Table 1
Population parameters of EC_a, soil textural fractions and water infiltration; n = number of samples, s^2 = variance.

Variable	n	Minimum	Maximum	Mean	s^2
EC_a-d [mS m^{-1}]	14 125	27	43	35.7	19.1
EC_a-i [mS m^{-1}]	14 125	36	44	39.4	9.4
Sand [%]	65	12	65	43	24.2
Silt [%]	65	30	69	47	12.8
Clay [%]	65	4	20	11	5.7
Infiltration rate [mm day^{-1}]	65	15	33	23	15.0

classified into groups using a fuzzy k-means classification procedure. Therefore the FuzMe 3.0 software (Minasny and McBratney, 2006) based on the modified fuzzy k-means for predictive classification as described by de Gruijter and McBratney (1988) using the Mahalanobis distance matrix was used. The classification was guided by fuzziness performance index (FPI) and modified partition entropy (MPE) (McBratney and Moore, 1985) and the optimum number of classes was chosen where these two measures were minimal. FPI ($0 \leq FPI \leq 1$) is a measure of the degree of membership sharing among classes, where a value close to 1 indicates a strong sharing of membership and 0 represents crisp classes with no membership sharing. The MPE ($0 \leq MPE \leq 1$) estimates the degree of disorganization in the classification and a value close to 1 indicates a complete disorganization while 0 reflects perfect organization.

2.5. Water infiltration measurement and soil texture analysis

After land preparation and EC_a-i measurements, the soil was characterized at 65 locations: 30 locations were selected according to a grid to ensure equal coverage and the rest were randomly located.

At every location the infiltration rate was measured three times within 1 m^2 with a double ring infiltrometer (0.30 m inner ring diameter and 0.45 m outer ring) by measuring the decrease in water level in the inner ring as a function of time. Readings continued until the infiltration rate stabilized which was generally within two days.

After the infiltration measurements soil samples were taken at the same locations at a 0–0.30 m depth interval and the three replications obtained within each 1 m^2 were mixed. The three major textural fractions (clay: 0–2 μm, silt: 2–50 μm and sand: 50–2000 μm) were analyzed following the conventional sieve-pipette method.

3. Results and discussion

3.1. EC_a-data

Table 1 shows the population statistics of the EC_a measurements for both surveys. The mean EC_a-i (39.4 mS m^{-1}) was higher than that of EC_a-d (35.7 mS m^{-1}), which can be explained by the general increase in conductivity due to the water saturated conditions. Also a clear decrease in the variance was observed: 19.1 (mS m^{-1})^2 for EC_a-d and 9.4 (mS m^{-1})^2 for EC_a-i, indicating a twice as large variability within the EC_a-d data. So inundating the field resulted in less variable EC_a measurements with a larger signal–noise ratio. This clearly indicates the added value of mobile EC_a measurements in water saturated fields.

3.2. Variogram analysis and kriging

Fig. 2 shows the standardized experimental variograms and the fitted spherical models for EC_a-d and EC_a-i and Table 2 gives the parameters of fitted models. It can be observed that both variograms display a very similar behaviour in their structured part: the same model with almost identical ranges. However, the nugget

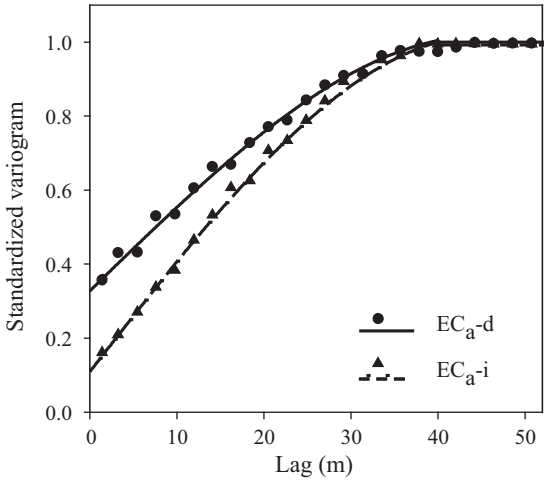

Fig. 2. Standardized experimental variograms (dots and triangles) and their spherical models (curves) of the EC_a-d and EC_a-i data.

variance was considerably higher for EC_a-d (32%) than for EC_a-i (10%), expressing more micro-variability or noise. Since the measurements were conducted with the same sensing system, this difference should be related to differences in the measurement conditions. Under dry conditions, the sensor platform was pulled over an uneven land surface with soil clods and crop stubbles, while under inundated condition the floating device experienced almost no shaking. Furthermore, the homogenous EC_a of the standing water layer under the inundated conditions might have contributed also in reducing the measurement variability and the nugget variance.

The interpolated maps of EC_a-d and EC_a-i showed similar patterns (Fig. 3a and b). The highest EC_a values were located in the north of the field while the lowest were found near the south-east and south-west corners. In general, both maps show patterns of fluctuating EC_a values with a similar trend.

3.3. EC_a and soil texture

Besides soil moisture, soil texture and organic matter (OM) play key roles in influencing EC_a measurements under non-saline conditions (Rhoades et al., 1999; Saey et al., 2009). Considering the shallow plough layer (approx. 0.15 m) of the paddy field and fibrous root growth pattern of paddy plants, soil beneath the ploughed layer is assumed to be poor in OM (Alam et al., 1993). Given that texture is a stable soil property, the spatial distribution of EC_a of both surveys was explained by the spatial variation of soil texture.

Table 2
Parameters of the standardized spherical variogram models for EC_a-d and EC_a-i.

Variable	C_0	C_1	a [m]
EC_a-d	0.32	0.68	41
EC_a-i	0.10	0.90	42

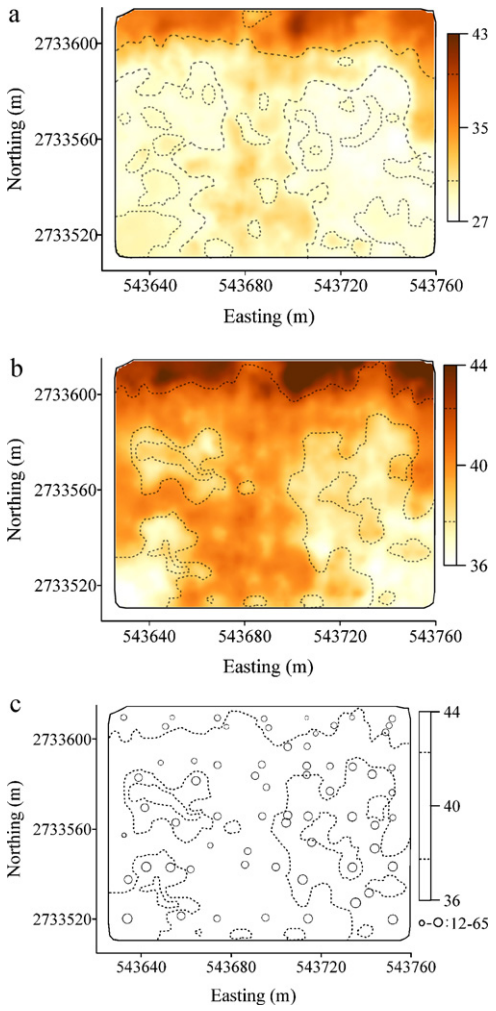

Fig. 3. The interpolated (a) EC_a-d [mS m^{-1}], (b) EC_a-i [mS m^{-1}] maps of the paddy field; the dashed lines indicate the upper and lower quartiles of EC_a data and (c) sand content [%] at the 65 locations, expressed as proportionate circles and plotted with the EC_a-i quartile lines. The co-ordinates are expressed in m, conforming to the Bangladesh Transverse Mercator projection with map datum Gulshan 303.

Table 1 provides the statistics of the textural analysis of the 65 soil samples. On average the topsoil has a loamy texture, but there is some variation and two more textural classes were encountered: sandy loam and silt loam (Fig. 4). Table 3 gives the correlation coefficients (r) between the soil textural fractions of the top 0.30 m and the EC_a measured under dry and inundated conditions of the 65 soil samples. The largest absolute r was found for the sand fraction, although the silt fraction showed a similar value. The correlation coefficients between all soil textural fractions and EC_a-i were stronger than with EC_a-d, which can be explained by the increased moisture variability under drained conditions. Fig. 3c shows a plot of the sand fraction projected on two contour lines of the EC_a-i map (Fig. 3b). The general relationship is clear: more sand was found where the EC_a-i is the smallest. So, the relationship between soil texture and EC_a was observed more accurately under inundated

Table 3
Pearson correlation coefficient (r) between EC_a-d and EC_a-i, and the textural fractions (n = 65).

Variable	Clay	Silt	Sand
EC_a-d	0.55	0.81	−0.83
EC_a-i	0.56	0.84	−0.86

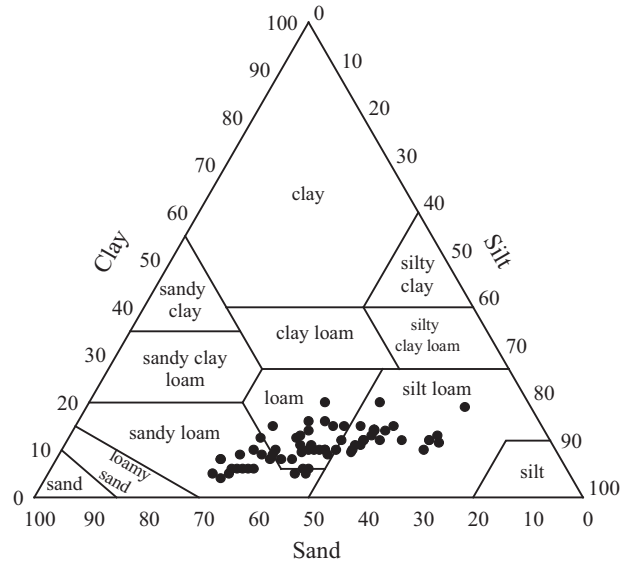

Fig. 4. Soil texture analysis of 65 locations plotted on the USDA soil texture triangle.

conditions because of the more homogeneous moisture conditions and the increased stability of the sensing platform.

Considering the stronger relation between EC_a-i measurements and soil texture, the EC_a-i data were classified to delineate EC_a classes using the fuzzy k-means algorithm. During classification, both FPI and MPE decreased until an optimum combination was found which was identified as two. Fig. 5 shows these two classes: class-1 grouped high EC_a values with a centroid value of 42.1 mS m^{-1} and class-2 the low EC_a values with a centroid value of 38.3 mS m^{-1} (areas less than 10 m^2 were merged with the surrounding class for practical reasons). These delineated EC_a classes were considered as different entity having significance for soil–water percolation behaviour of the field.

3.4. Water infiltration

The statistics of the 65 infiltration measurements are given in Table 1. The mean infiltration rate was 23 mm day^{-1}, which is very low. Yet at some locations a value of 15 mm day^{-1} was found where at another it increased to 33 mm day^{-1}. To investigate the link between water infiltration and EC_a, the 65 observations of the infiltration rate were grouped according to the EC_a classes. Table 4 gives the summary statistics together with a statistical comparison of the mean values of these classes. A significantly lower mean infiltration rate was found in EC_a class-1, i.e. the class with the higher EC_a

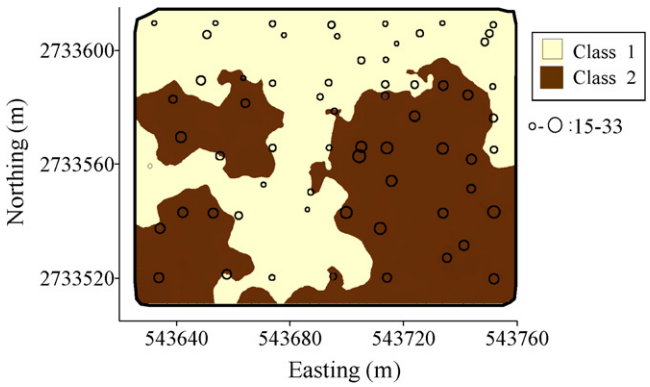

Fig. 5. Map of the EC_a classes obtained by fuzzy k-means classification; infiltration rates [mm day^{-1}] at the 65 locations are expressed as proportionate circles.

Table 4
Statistical parameters of the EC_a classes; n = number of samples per EC_a class, s = standard deviation.

Variable	EC_a class	n	Mean*	s
EC_a-i [mS m^{-1}]	Class-1	7769	41.9	2.1
	Class-2	6356	37.7	2.7
Infiltration rate [mm day^{-1}]	Class-1	37	19	2.1
	Class-2	28	27	2.7
Sand [%]	Class-1	37	34	4.8
	Class-2	28	54	5.3
Silt [%]	Class-1	37	53	3.8
	Class-2	28	38	3.1
Clay [%]	Class-1	37	13	1.7
	Class-2	28	8	1.3

* Means of classes are significantly different ($p = 0.05$) according to Fisher's least significant difference test.

values, while the infiltration rate was significantly higher for EC_a class-2, having lower EC_a values. So in general, water infiltration rate followed the opposite trend of the EC_a values, i.e. the lower the EC_a, the higher the infiltration. This is also illustrated by the infiltration values plotted in Fig. 5. Since EC_a class-2 had the larger water infiltration values and higher sand fraction than class-1, it can be reasonably assumed that both are related. The significant difference of the other two soil textural fractions between the two classes also indicates this relationship. Higher fine textural fractions (silt and clay) in class-1 significantly reduced water infiltration and vice versa.

4. Conclusions

We used successfully an EMI based Floating Sensing System to measure in detail the soil EC_a variation beneath the standing water of an inundated paddy field. Although both dry and inundated surveys showed a similar spatial structure of the EC_a values, the EC_a-i measurements were less variable with a larger signal–noise ratio because the sensing platform could be operated in a more stable way and the uniform moisture status of the field reduced the effect of moisture variability on EC_a measurements. As a result, the EC_a response from the inundated field condition was stronger correlated to the soil texture fractions (mainly with the sand fraction). The EC_a-i survey values were grouped into two EC_a classes with a significant difference in water infiltration: class-1 with higher EC_a values had a significantly lower average water infiltration rate than class-2. The delineated zones can be considered as separate units for soil–water management, hence allowing optimization of water resources during land preparation and irrigation.

It can be concluded that an EMI-based Floating Sensing System is useful in delineating within-field zones to support the evaluation of soil–water relationship. This can have further significance in floodplains and wet-land agriculture systems where zone based crop irrigation-drainage regimes can be introduced to promote optimization of benefits from site specific soil–water management practices.

References

Alam, M.L., Saheed, S.M., Shinagawa, A., Miyauchi, N., 1993. Chemical Properties of General Soil Types of Bangladesh, vol. 29. Memoirs of the Faculty of Agriculture, Kagoshima University, pp. 75–87.

Bouman, B.A.M., Tuong, T.P., 2001. Field water management to save water and increase its productivity in irrigated lowland rice. Agric. Water Manage. 49, 11–30.

Brammer, H., 1981. Reconnaissance Soil Survey of Dhaka District, Revised edition. Soil Resources Development Institute, Dhaka, Bangladesh, pp. 6–19.

Brammer, H., 1996. The Geography of the Soils of Bangladesh. The University Press Limited, Dhaka 1000, Bangladesh, p. 25.

Brevik, E.C., Fenton, T.E., Lazari, A., 2006. Soil electrical conductivity as a function of soil water content and implications for soil mapping. Precis. Agric. 7, 393–404.

de Gruijter, J.J., McBratney, A.B., 1988. A modified fuzzy *k*-means method for predictive classification. In: Bock, H.H. (Ed.), Classification and Related Methods of Data Analysis. Elsevier, Amsterdam, pp. 97–104.

Goovaerts, P., 1997. Geostatistics for Natural Resources Evaluation. Oxford University Press, New York.

Islam, M.M., Van Meirvenne, M., 2011. FloSSy: a Floating Sensing System to evaluate soil variability of flooded paddy fields. In: Stafford, J.V. (Ed.), Proceedings of the 8th European Conference on Precision Agriculture. University of Life Sciences, Prague, Czech Republic, pp. 60–66.

Islam, M.M., Meerschman, E., Cockx, L., De Smedt, P., Meeuws, F., Van Meirvenne, M., 2011a. Comparison of apparent electrical conductivity measurements on a paddy field under flooded and drained conditions. In: Stafford, J.V. (Ed.), Proceedings of the 8th European Conference on Precision Agriculture. University of Life Sciences, Prague, Czech Republic, pp. 43–50.

Islam, M.M., Cockx, L., Meerschman, E., De Smedt, P., Meeuws, F., Van Meirvenne, M., 2011b. A Floating Sensing System to evaluate soil and crop variability within flooded paddy rice fields. Precis. Agric., doi:10.1007/s11119-011-9226-5.

McBratney, A.B., Moore, A.W., 1985. Application of fuzzy sets to climate classification. Agric. For. Meteorol. 35, 165–185.

McNeill, J.D., 1980. Electromagnetic Terrain Conductivity Measurement at Low Induction Numbers. Technical Note TN-6. Geonics Limited, Missisauga, Ontario, Canada.

Minasny, B., McBratney, A.B., 2006. FuzME Version 3. Australian Centre for Precision Agriculture, the University of Sidney, NSW.

Rhoades, J.D., Chanduvi, F., Lesch, S.M., 1999. Soil Salinity Assessment: Methods and Interpretation of Electrical Conductivity Measurements. FAO Rep. 57. FAO, Rome, Italy.

Saey, T., Simpson, D., Vermeersch, H., Cockx, L., Van Meirvenne, M., 2008. Comparing the EM38DD and DUALEM-21S sensors for depth-to-clay mapping. Soil Sci. Soc. Am. J. 73, 7–12.

Saey, T., Van Meirvenne, M., Vermeersch, H., Ameloot, N., Cockx, L., 2009. A pedotransfer function to evaluate the soil profile textural heterogeneity using proximally sensed apparent electrical conductivity. Geoderma 150 (3–4), 389–395.

Sheets, K.R., Hendrickx, J.M.H., 1995. Non-invasive soil water content measurement using electromagnetic induction. Water Resour. Res. 31, 2401–2409.

Sudduth, K.A., Hummel, J.W., Birrell, S.J., 1997. Sensors for site-specific management. In: Pierce, F.J., Sadler, E.J. (Eds.), The State of Site-Specific Management for Agriculture. ASA-CSSA-SSSA, Madison, WI, USA, pp. 183–210.

Yoshida, S., 1983. Rice. In: Smith, W.H., Banta, S.J. (Eds.), Potential Productivity of Field Crops Under Different Environments. International Rice Research Institute, Los Banos, Philippines.